Available online at www.sciencedirect.com
SCIENCE DIRECT®
Analytica Chimica Acta 491 (2003) 47–56
ANALYTICA CHIMICA ACTA
www.elsevier.com/locate/aca

Determination of carbendazim, fuberidazole and thiabendazole by three-dimensional excitation–emission matrix fluorescence and parallel factor analysis

M.J. Rodríguez-Cuesta [a,*], R. Boqué [a], F.X. Rius [a], D. Picón Zamora [b], M. Martínez Galera [b], A. Garrido Frenich [b]

[a] *Department of Analytical and Organic Chemistry, Institute of Advanced Studies, Chemometrics and Qualimetrics Group, Rovira i Virgili University, Pça. Imperial Tàrraco, 1, 43005 Tarragona, Spain*
[b] *Department of Hydrogeology and Analytical Chemistry, University of Almería, 04071 Almeria, Spain*

Received 17 April 2003; received in revised form 10 June 2003; accepted 20 June 2003

Abstract

We simultaneously determined carbendazim, fuberidazole and thiabendazole by excitation–emission matrix (EEM) fluorescence in combination with parallel factor analysis (PARAFAC). Three-way deconvolution provided the pure analyte spectra from which we estimated the selectivity and sensitivity of the pesticides, and the relative concentration in the mixtures from which we established a linear calibration. Special attention was given calculating such figures of merit as precision, sensitivity and limit of detection (LOD), derived from the univariate calibration curve. The method, which had a relative precision of around 2–3% for the three pesticides, provided limits of detection of 20 ng ml^{-1} for carbendazim, 4.7 ng ml^{-1} for thiabendazole and 0.15 ng ml^{-1} for fuberidazole. The accuracy of the method, evaluated through the root mean square error of prediction (RMSEP), was 27.5, 1.4, and 0.03 ng ml^{-1}, respectively, for each of the pesticides.
© 2003 Elsevier B.V. All rights reserved.

Keywords: Three-way calibration; PARAFAC; Figures of merit; Excitation–emission matrix fluorescence

1. Introduction

Pesticides are polluting compounds whose concentration is regulated by the European Commission in many samples such as drinking waters. Traditionally, instrumental techniques to determine these compounds involve gas (EPA method 515.1) or liquid chromatography (EPA method 531.1, 632 and 8318). Fluorimetric techniques can also be used to analyse pesticides in mixtures since many pesticides, including the ones studied in this paper, are intrinsically fluorescent. Fluorescence spectroscopy is a versatile analytical technique, which provides high sensitivity of detection. However, in multicomponent mixtures the fluorescence signal is normally overlapped and chemical procedures (in few cases) or chemometrical techniques of resolution have to be applied if it is to be quantitatively analysed. One of the mathematical resolution strategies is the collection of an entire excitation–emission matrix (EEM) fluorescence spectrum combined with multi-way deconvolution and calibration algorithms. In this way, Picón Zamora et al. [1] determined three pesticides by taking linear trajectories across the EEM and applying principal

* Corresponding author. Tel.: +34-977-558122; fax: +34-977-559563.
E-mail address: cuesta@quimica.urv.es (M.J. Rodríguez-Cuesta).

0003-2670/$ – see front matter © 2003 Elsevier B.V. All rights reserved.
doi:10.1016/S0003-2670(03)00786-4

component regression (PCR) and partial least squares (PLS1 and PL2) algorithms; Saurina et al. [2] resolved the EEM of triphenyltin in synthetic and natural sea water samples with multivariate curve resolution (MCR); and JiJi et al. [3] determined carbamate pesticides by parallel factor analysis (PARAFAC) of the excitation–emission matrix. We applied a procedure similar to this latter one, and paid particular attention to the internal validation of the method and to the calculation of the figures of merit.

We determined carbendazim, fuberidazole and thiabendazole in mixtures of the three pesticides by PARAFAC deconvolution of the three-dimensional excitation–emission data. Internal validation was assessed from the correlation between the pure excitation and emission spectra of each compound, and the reference spectra, as a measure of the reliability of the model. The selectivities of the three pesticides were calculated from the recovered spectra. Next, a univariate regression was performed for each pesticide by relating the loadings of the PARAFAC decomposition with the known concentrations of the pesticides in the calibration samples. From these univariate calibration lines, figures of merit such as precision, sensitivity and limit of detection (LOD) were calculated. The effect of the spectral selectivities on these figures of merit is also discussed. Finally, the accuracy of the method was estimated by predicting a new set of samples, which were not included in the calibration step.

2. Theory

2.1. Three-way decomposition of fluorescence data

Fluorescence three-way data can be decomposed by parallel factor analysis because each analyte in the sample can ideally be described by one PARAFAC component [4]. This means that each fluorophore's contribution to the emission is independent of the contribution of the remaining fluorophores and identical for different samples (only varying in proportions). Hence, the PARAFAC model for a three-way array (x_{ijk}) can be denoted as:

$$x_{ijk} = \sum_{f=1}^{F} a_{if}\, b_{jf}\, c_{kf} + e_{ijk} \qquad (1)$$

In the case of excitation–emission matrix fluorometry, the kth slice of the trilinear cube $\underline{\boldsymbol{X}}$ is the $(I \times J)$ matrix of excitation and emission profiles of the fluorescent components for the kth sample. Thus, a_{if}, b_{jf} and c_{kf} are the typical elements of the loading matrices $\boldsymbol{A}$, $\boldsymbol{B}$ and $\boldsymbol{C}$ (emission wavelength, excitation wavelength and relative concentrations in the samples, respectively) for a given number of components F. Using an alternate least squares (ALS) procedure, the trilinear model is found to minimise the sum of squares of the residuals e_{ijk}. In matrix notation, and using the Khatri–Rao product [5], the PARAFAC model can be formulated in terms of the unfolded array as shown in Eq. (2):

$$\underbrace{\boldsymbol{X}_k}_{(IJ\times K)} = (\underbrace{\boldsymbol{B}}_{(J\times F)} | \otimes | \underbrace{\boldsymbol{A}}_{(I\times F)}) \underbrace{\boldsymbol{C}^{\mathrm{T}}}_{(K\times F)} = \underbrace{\boldsymbol{Z}}_{(IJ\times F)} \boldsymbol{C}^{\mathrm{T}} \qquad (2)$$

An important characteristic of the PARAFAC model is the uniqueness of its solution. This means that additional constraints, such as orthogonality or external information to solve rotational freedom are not needed to identify the model [6]. This property is an extension of the second-order advantage and so trilinear data (here fluorescence data) can be calibrated when there are unknown interferences in the samples.

In dilute solutions or suspensions, fluorescence intensity is linearly proportional to the solute concentration, and fluorescent excitation–emission measurements follow a trilinear model, such as the PARAFAC [5,7–9]. However, spectral properties are affected by the local environment. The most common environmental factors that influence fluorescence properties are solvent polarity, pH and fluorescence quenching (*quenching* is any process which decreases the fluorescence intensity of a sample, e.g. excited-state reactions, molecular rearrangements, energy transfer, ground–state complex formation and collision quenching, such as the one produced by molecular oxygen) [10].

Despite this environmental influence, fluorescence measurements can still fulfil the trilinear model if we keep the conditions constant throughout the experiments. However, other problems cannot be so effectively handled by PARAFAC based models. One of these is the emission region below excitation, where the intensity is approximately zero, i.e. the fluorophore shows no fluorescence. Whether these data

are recorded or not, they should be treated as missing values and cannot be replaced with zeros to prevent the PARAFAC model from trying to fit them [5,11]. Other potential problems are Rayleigh and Raman scattering. Raman interference due to the solvent can often be almost completely removed by subtracting the solvent spectra from the sample spectra. Rayleigh scattering occurs in the EEM when the excitation wavelength is equal to the emission wavelength and there are no intrinsic profiles in either the *X*- or *Y*-order to extract. Several strategies for solving this problem have been described in the literature (e.g. data analysis can be restricted to regions were the scattering does not appear, a blank spectra can be subtracted if available or the data points can be weighed) [7,12].

2.2. PARAFAC calibration and prediction

The decomposition of the three-way data by PARAFAC gives rise to three loading matrices, one of which, $\boldsymbol{C}$, corresponds to the sample mode. The $\boldsymbol{C}$-loadings are the relative concentrations of the pesticides in the mixtures. In the calibration step, these loadings are regressed against the real concentrations of each pesticide in the mixtures to get a linear calibration line [2]. In the prediction step, this regression line can then be used to predict (if any new interferent is present) the concentration of each pesticide in future test samples, $\boldsymbol{X}_{\text{un}}$ that are not in the initial calibration dataset, by interpolating their loadings of relative concentration, $\boldsymbol{C}^{\text{T}}$. These loadings can be previously calculated from the Eq. (2) multiplying the pseudoinverse of the $\boldsymbol{Z}$ matrix by the test sample data, as shows Eq. (3):

$$\boldsymbol{C}^{\text{T}} = (\boldsymbol{Z}^{\text{T}}\boldsymbol{Z})^{-1}\boldsymbol{Z}^{\text{T}}\boldsymbol{X}_{\text{un}} \quad (3)$$

Another way to predict future test samples is to include them in the initial PARAFAC model. In this way, the loading matrices for both the calibration and the prediction sets are recovered. All the samples are considered to calculate the model parameters although the regression fit is only performed with the calibration samples. Finally, the loadings of the PARAFAC model for the prediction samples are interpolated into the corresponding regression line to obtain the predicted concentration of each analyte.

3. Experimental

3.1. Samples and standards

To determine the pesticides in synthetic samples, a set of 12 mixtures was prepared in methanol between 0 and 100 ng ml^{-1} for carbendazim, 0–0.7 ng ml^{-1} for fuberidazole and 0–40 ng ml^{-1} for thiabendazole. A standard of each pure pesticide was also prepared (Table 1).

Excitation–emission fluorescence matrices were recorded for all the standards. In each experiment, a methanol blank was subtracted to remove the interfering Raman effect of the solvent.

3.2. Instrumentation and data analysis

Measurements were performed with an Aminco–Bowman Series 2 luminescence spectrometer equipped with a 150 W continuous xenon lamp. The EEM were defined so that they would collect the variation in the signal caused by the pesticides, and not record either excitation signals below emission or Rayleigh scattering. The dimension of the data matrices was 50 × 38, from 310 to 370 nm in the emission domain and from 260 to 306 nm in the excitation domain. The excitation and emission slits were both maintained at 4 nm and the scanning rate was 7 nm s^{-1}. All

Table 1
Concentration of the pesticides in the synthetic mixtures and individual standards

Sample	Carbendazim (ng ml^{-1})	Thiabendazole (ng ml^{-1})	Fuberidazole (ng ml^{-1})
Ml	0	20	0.4
M2	50	20	0.0
M3	50	0	0.4
M4	30	30	0.5
M5	60	35	0.6
M6	20	15	0.1
M7	100	25	0.2
M8	90	35	0.4
M9	40	25	0.4
M10	60	20	0.5
M11	80	40	0.1
M12	90	35	0.3
Carbendazim	75	0	0.0
Fuberidazole	0	0	0.7
Thiabendazole	0	35	0.0

measurements were performed in a 10 mm quartz cell at 750 V.

An AB2 software version 1.40, running under OS/2 2.0 was used for spectral acquisition and MATLAB 6.0 (The MathWorks Inc., 2000) was used for data analysis. In the Matlab environment, commercial [13] and home-made algorithms were used to process the data.

4. Results and discussion

4.1. Preliminary study of the data

A preliminary principal component analysis (PCA) can provide information about the degree of correlation of the data and the presence of outliers or influential samples. So we unfolded column-wise the EEM of each sample to a row vector of 1900 elements, and use them to build a new data matrix of 12 rows (samples) and 1900 columns (wavelengths). The dimensionality of the data was reduced with the unfold-PCA to two factors, which explained 97% of the variation in the data. In spite of there being three components, the high correlation between the fluorescence spectra explains the presence of only two significant principal components. Fig. 1 shows the PC1–PC2 scores plot (explained variance is 86 and 11%, respectively) and the influence plot (squared residuals on X versus leverage). We can observe that sample M12 is far from the centre in the scores plot and has a high leverage value, which indicates that it is an influential sample.

A PARAFAC model with three factors was also performed with the whole set of mixtures to get an idea of the distribution of the samples. We represented the loadings of the sample mode in two dimensions and observed that M12 was again the most different sample, according to the U-PCA results.

4.2. Individual standards

Fig. 2 shows the excitation and emission spectra obtained for each pesticide. They were obtained by applying PARAFAC with one factor and non-negativity constraints to the three-dimensional matrices for the individual fluorescence spectra of each pesticide. We regarded these normalised profiles as the spectra of the *pure* pesticides and used them as reference spectra to evaluate the reliability of the models in the calibration.

In a preliminary study [1], some of the authors recorded the pure excitation and emission spectra at the wavelengths of maximum emission and excitation, respectively. Correlation between those spectra and the ones in this paper, resolved by PARAFAC on the EEM of the individual pesticides, was higher than 0.998.

We calculated the sensitivity and selectivity of the pesticides from their first-order profiles in both the excitation and the emission region (see Table 2). All figures of merit were calculated as described by Faber et al. [14]. In terms of first-order profiles, fuberidazole was the most sensitive compound, both in the excitation and the emission region, but one of the least selective, together with thiabendazole. The most selective pesticide was carbendazim, as its spectra are the most different in shape (see Fig. 2) and therefore the least correlated. This preliminary information suggests that fuberidazole will be predicted at lower concentrations (it is the most sensitive) but with a higher error of prediction because it is highly correlated with thiabendazole. It also suggests that carbendazim will be the most accurately predicted because of its selectivity.

4.3. Calibration step

In the calibration step, we performed several PARAFAC models, which consisted of different calibration samples, and not necessarily the individual standards of each pesticide.

The models that included the individual standard of carbendazim in the calibration set recovered the profiles slightly better than the models that did not.

Table 2
First-order sensitivities and selectivities of carbendazim, thiabendazole and fuberidazole, estimated from the standards of the pure pesticides[a]

	Compound	Sensitivity	Selectivity
$\boldsymbol{X}$ (50 × 3) emission spectra	Carbendazim	15.45	0.8068
	Thiabendazole	19.19	0.1976
	Fuberidazole	356.5	0.2073
$\boldsymbol{Y}$ (38 × 3) excitation spectra	Carbendazim	7.635	0.3985
	Thiabendazole	11.23	0.1157
	Fuberidazole	240.9	0.1401

[a] Figures of merit for first-order spectral profiles.

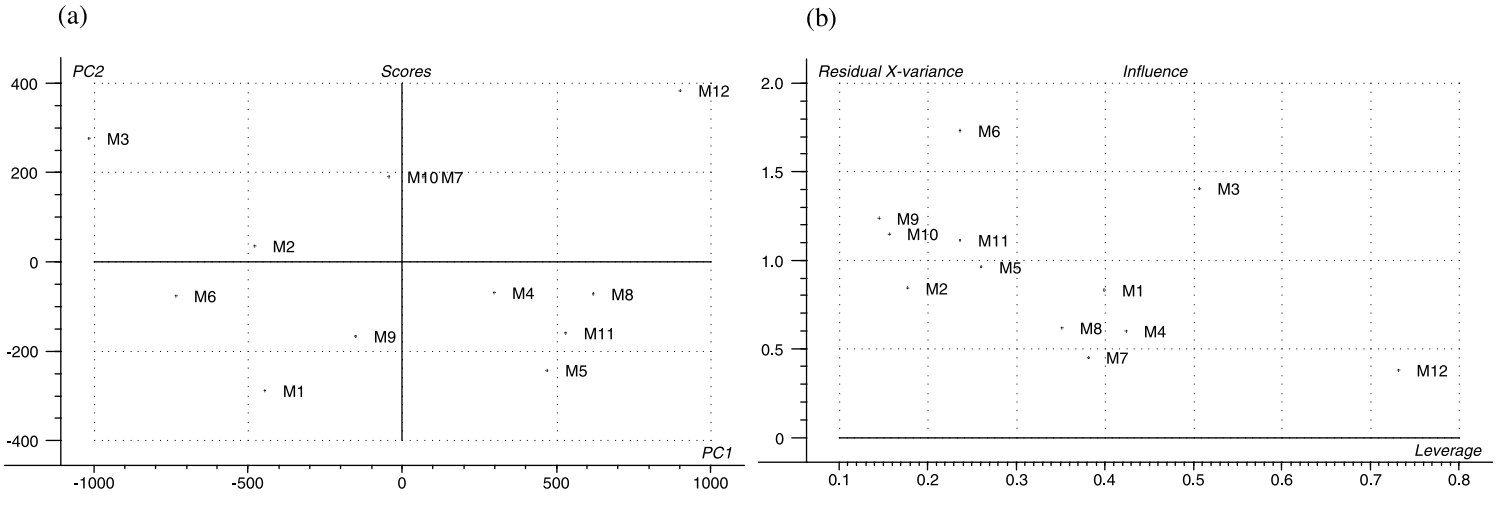

Fig. 1. Scores (a) and influence (b) plot from the PCA of the columnwise unfolded matrices corresponding to the 12 synthetic mixtures (explained variance 97%).

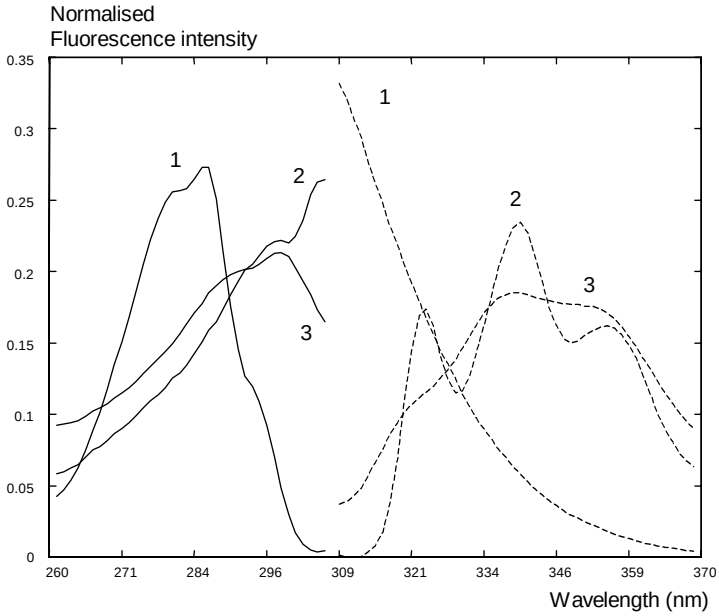

Fig. 2. Excitation (solid lines) and emission (broken lines) spectra of (1) carbendazim (50 ng ml^{-1}), (2) fuberidazole (0.7 ng ml^{-1}) and (3) thiabendazole (35 ng ml^{-1}).

The same occurred with the standard of thiabendazole. However, the presence of the standard of fuberidazole considerably improved the recovery of the profiles and, therefore, the correlation between them and the reference spectra. In the models which did not contain fuberidazole, on the other hand, the profiles of each pesticide could not be unequivocally identified. This is due to the sensitivity and selectivity values of the compounds. When mixtures of three analytes were analysed by fluorescence, and the data were modelled by PARAFAC, the standard of the most selective and sensitive analytes did not have to be included, because the model was able to recover their profiles in the presence of other analytes. This was the case of carbendazim. However, thiabendazole and fuberidazole are less selective and highly correlated each other, so the model needs extra information (such as the individual standard) about the most sensitive of them (fuberidazole, in this case), so that the profiles can be reliably recovered.

The best calibration set consisted of the calibration samples located at the extremes of the domain, i.e. M2, M5, M7 and M11 (extrapolation out of the linear range is avoided) together with the individual standard of fuberidazole (see above). This PARAFAC model was built with three factors and non-negativity constraints in all the modes. The estimated profiles matched the reference spectra (see Fig. 3), with correlation coefficients of 0.996 for carbendazim, 0.998 for thiabendazole and 1.000 for fuberidazole in the excitation region and 0.9995, 0.996 and 1.000, respectively, in the emission region.

Table 3 shows the figures of merit of this model. They were calculated, using univariate statistics, from the calibration line fitted with the loadings in the sample mode obtained with PARAFAC, as explained above.

Sensitivity was defined as the slope of the calibration curve. The values of this sensitivity measure correlate well with those calculated from the net analyte signal of the first-order spectra of each pesticide. Other authors have suggested a single measure of sensitivity for PARAFAC models based on net analyte signal calculations [15]. From the results of Table 3 we can conclude that fuberidazole is the most sensitive compound in the mixture, followed by thiabendazole and carbendazim, in agreement with the spectroscopic data from Table 2.

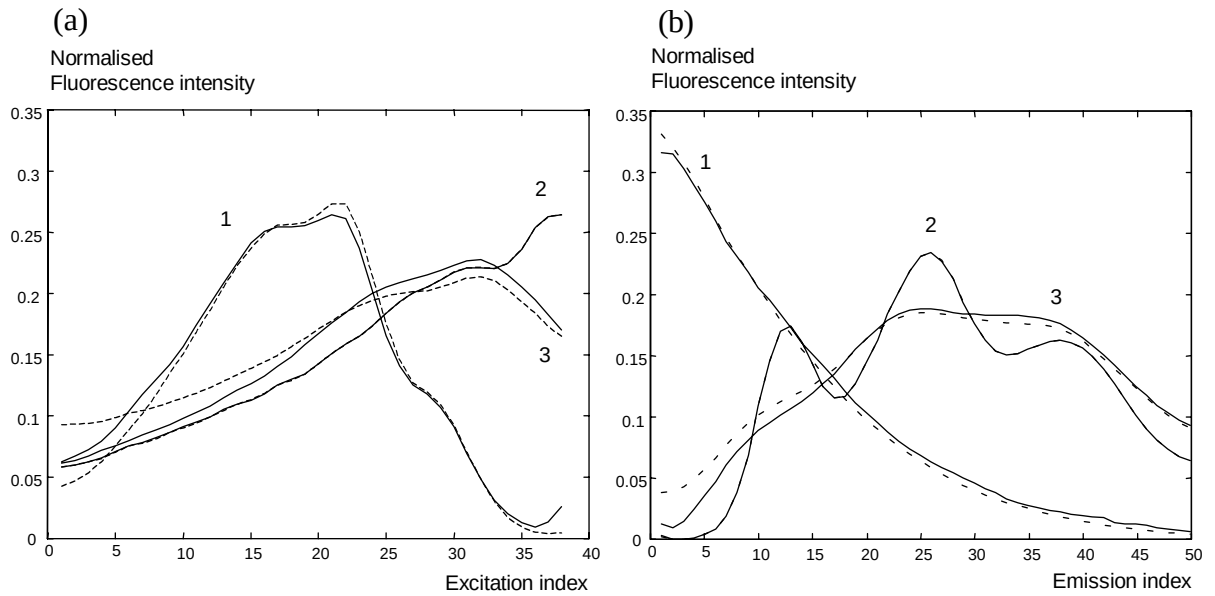

Fig. 3. (a) Excitation and (b) emission spectra for carbendazim (1), fuberidazole (2) and thiabendazole (3). Broken lines: reference spectra; solid lines: spectra recovered by the PARAFAC model.

The precision for each pesticide was calculated in terms of concentration as the standard deviation of the $\boldsymbol{C}$-loading residuals for all standards divided by the sensitivity, SEN, i.e. the slope of the calibration line as:

$$\text{precision} = \frac{s_{\text{res}}}{\text{SEN}} = \text{SEN}^{-1}\sqrt{\frac{\sum_{i=1}^{n}(c_i - \hat{c}_i)^2}{n-2}} \quad (4)$$

c_i are the $\boldsymbol{C}$-loadings for the given pesticide estimated from the PARAFAC model and $\hat{c}_i$ are the loadings estimated from the calibration line $\boldsymbol{C}$-loadings versus pesticide concentration. n is the number of calibration standards.

Finally, the LOD for each pesticide was estimated from Eq. (5), which takes into account the uncertainty of the calibration line and considers α and β probabilities of error, following the IUPAC recommendations [16]:

$$\text{LOD} = \delta(\alpha, \beta)\frac{s_{\text{res}}}{\text{SEN}}\sqrt{1 + \frac{1}{n} + \frac{\bar{x}^2}{\sum_{i=1}^{n}(x_i - \bar{x})^2}} \quad (5)$$

Table 3
Statistical parameters and figures of merit of the linear relationship between the proportion loadings calculated by PARAFAC and the true concentration of each pesticide

	Carbendazim	Thiabendazole	Fuberidazole
Number of data points	5	5	4
Intercept	9.34×10^{-3}	-9.37×10^{-3}	-3.78×10^{-3}
Sensitivity (slope)	6.54×10^{-3}	16.4×10^{-3}	349.3×10^{-3}
Standard deviation of intercept	19.9×10^{-3}	11.9×10^{-3}	5.80×10^{-3}
Standard deviation of slope	2.96×10^{-4}	4.27×10^{-4}	181.3×10^{-4}
Standard error	22.3×10^{-3}	13.3×10^{-3}	8.26×10^{-3}
Correlation coefficient (r)	0.9969	0.9990	0.9973
Precision (%)	3.4	2.0	3.4
Limit of detection (ng ml^{-1})	20	4.7	0.15

x_i is the concentration of the given pesticide in the ith standard and $\bar{x}$ is the average concentration of the calibration standards.

The values of the correlation coefficients indicate the quality of the linear fits and the estimated precision shows that the calibration results are in close agreement. The detection limits of this method are in the order of magnitude of nanograms milliliters^{-1} (ng ml^{-1}). Expressed as a percentage of the higher analyte concentration in samples, they were around 20% for carbendazim and fuberidazole and below 12% for thiabendazole.

In order to test the second calibration strategy described in Section 2, we also performed the PARAFAC model with the chosen samples M2, M5, M7, M11, the standard of fuberidazole and the remaining samples to be predicted. We obtained the loadings of relative concentration for each sample, although the calibration line was fitted only with the calibration set. Table 4 shows the statistical parameters obtained for this regression. The estimated profiles were correctly recovered but the correlation coefficients with the reference spectra were slightly lower than those obtained with the model that did not include the prediction samples. This second model finds the solution that best explains all the variations, so we could not detect any outlying samples. Precision and limits of detection were of the same order for thiabendazole and higher for carbendazim and fuberidazole than with the previous model.

4.4. Prediction step

We used the PARAFAC model built with the calibration set [M2, M5, M7, M11, Fub] to predict the concentration of carbendazim, thiabendazole and fuberidazole in the prediction set consisting of the remaining samples in Table 1. For each pesticide, we interpolated the estimated PARAFAC $\boldsymbol{C}$-loadings, calculated from Eq. (3), in the corresponding regression line (see Table 3) and calculated the predicted concentration.

Fig. 4 shows the calibration model with a straight line, and the prediction samples indicated with crosses. The prediction results for thiabendazole and fuberidazole are very good. The accuracy of the models was calculated by the root mean square error of prediction (RMSEP):

$$\mathrm{RMSEP} = \sqrt{\frac{\sum_{i=1}^{m}(x_i - \hat{x}_i)^2}{m}} \tag{6}$$

where x_i and $\hat{x}_i$ are the measured and predicted concentrations of the given pesticide in the ith prediction sample, and m is the number of prediction samples. RMSEP was 3.4% for thiabendazole and 3.9% for fuberidazole. However, in the prediction of carbendazim, samples M4, M10 and M12 behaved very differently from the model and the rest of the samples and increased the RMSEP from 5.6 to 27.5%. Work is in progress to efficiently detect and handle outliers in prediction for PARAFAC models.

We also expressed these values in terms of recovery (as the percentage ratio between the predicted and the true concentration) so that they could be compared with those obtained by the procedure described in a previous study using multivariate calibration methods [1] (Table 3, Model C). The average recoveries for the PARAFAC procedure were 103.6% for thiabendazole,

Table 4
Statistical parameters and figures of merit of the linear relationship between the loadings of calibration samples obtained from a PARAFAC that includes the prediction samples (see details in text)

	Carbendazim	Thiabendazole	Fuberidazole
Number of data points	5	5	4
Intercept	2.01×10^{-3}	-4.45×10^{-3}	-7.37×10^{-3}
Sensitivity (slope)	42.8×10^{-3}	10.45×10^{-3}	326.9×10^{-3}
Standard deviation of intercept	14.1×10^{-3}	70.7×10^{-3}	103.1×10^{-3}
Standard deviation of slope	2.10×10^{-3}	2.55×10^{-3}	32.2×10^{-3}
Standard error	15.9×10^{-3}	7.94×10^{-3}	14.7×10^{-3}
Correlation coefficient (r)	0.9964	0.9991	0.9905
Precision (%)	3.7	1.9	6.4
Limit of detection (ng ml^{-1})	22	4.4	0.29

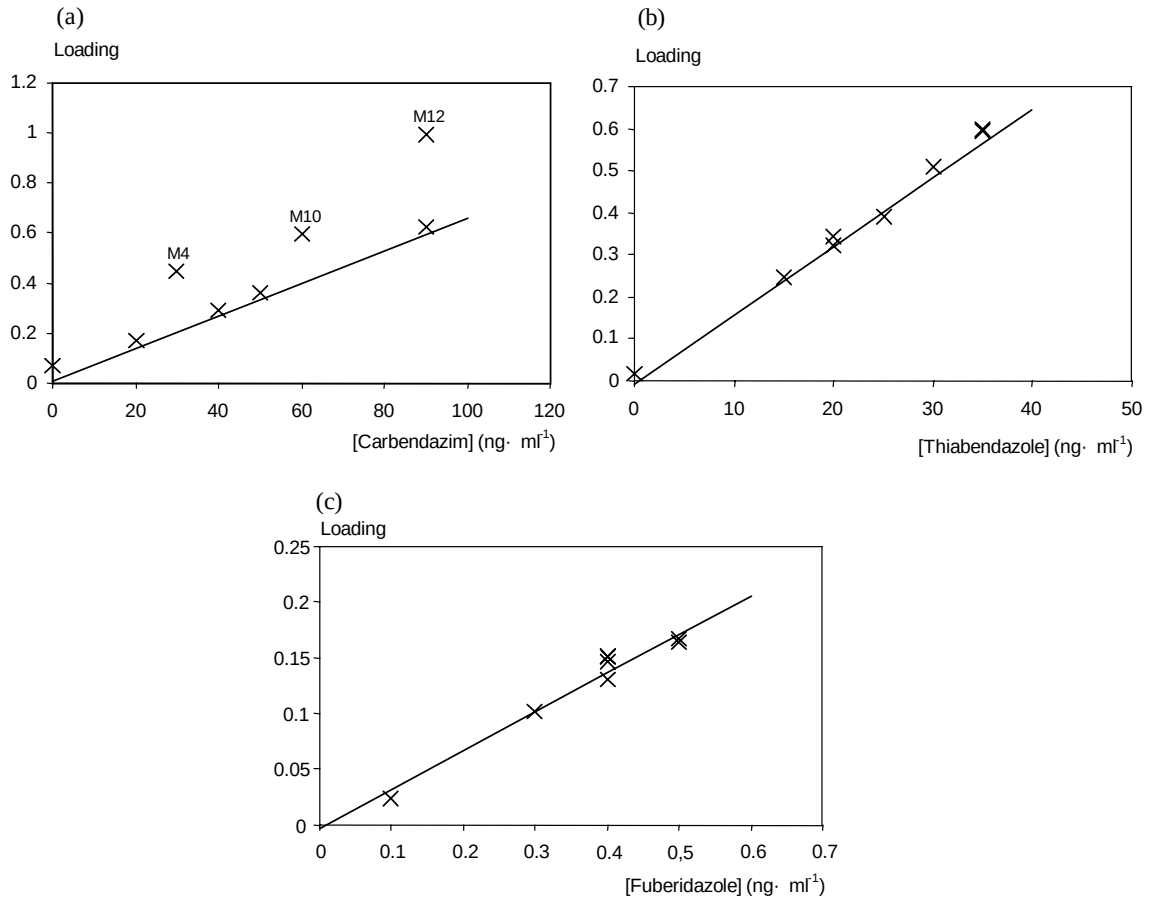

Fig. 4. Calibration graphs (straight line) for carbendazim (a), thiabendazole, (b) and fuberidazole (c). The crosses (×) represent the prediction samples.

99.9% for fuberidazole and 111.1% for carbendazim. For the multivariate calibration procedure they were 97.7% for thiabendazole, 93.3% for fuberidazole and 102.3% for carbendazim. So, in all the cases, recoveries were around the ideal 100% for both methods, although the dispersion of the results was lower for PARAFAC than for the multivariate calibration procedure.

However, the methodology involving PARAFAC did not require as many calibration samples as the PLS models do and, what is more, would allow the determination of any of the three pesticides in the presence of unknown interferences (second-order advantage) even if they were not included in the model.

We also predicted the samples in the prediction set by including them in the PARAFAC model. The loadings estimated from the PARAFAC model were interpolated into the calibration line that was fitted only with the loadings of the calibration samples. In

Table 5
Prediction errors of the two PARAFAC calibration procedures (see details in text)

RMSEP (%)	Carbendazim	Thiabendazole	Fuberidazole
PARAFAC (calibration set)	5.6	3.4	3.9
PARAFAC (calibration + prediction sets)	3.7	4.8	6.4

this way, anomalous samples went unnoticed and the RMSEP values were higher than those obtained by prediction from Eq. (3) (see Table 5). What is more, we would have to rebuild the model for each new set of prediction samples, which is less practical in a real laboratory situation.

5. Conclusions

We determined carbendazim, fuberidazole and thiabendazole in mixtures of the three pesticides, by EEM fluorescence and three-way PARAFAC calibration. We used two main criteria for selecting the calibration standards. Firstly, the model had to cover the experimental domain, so standards were preferably taken at the extremes of the domain to avoid subsequent extrapolation. Secondly, we used the selectivity and sensitivity information about the compounds to select the calibration samples, and discussed whether it was necessary to include extra information (i.e. individual standards) in the model for the more sensitive or the less selective analytes in the mixtures.

In the light of the results, we selected for further study a calibration set with six samples: five combinations of extreme concentrations for each pesticide and an individual standard of fuberidazole. The prediction ability of this model compared favourably with the prediction ability of previous PLS models. PARAFAC calibration also required fewer samples and would make quantification possible even in the presence of uncalibrated interferents.

Finally, the PARAFAC models were validated by calculating the univariate figures of merit from the calibration curves that had been built by regressing the PARAFAC sample loadings to the pesticide concentrations. These figures of merit were also used to compare the quality of the different models.

Acknowledgements

The authors would like to thank the MCyT (Project No. BQU2000-1256) for financial support and the CIRIT of the Catalan Government for providing M.J. Rodríguez's doctoral fellowship.

References

[1] D. Picón Zamora, M. Martínez Galera, A. Garrido Frenich, J.L. Martínez Vidal, Analyst 125 (2000) 1167.
[2] J. Saurina, C. Leal, R. Campañó, M. Granados, M.D. Prats, R. Tauler, Anal. Chim. Acta 432 (2001) 241.
[3] R.D. JiJi, G.A. Cooper, K.S. Booksh, Anal. Chim. Acta 397 (1999) 61.
[4] R. Bro, The N-way online course on PARAFAC and PLS, 1998 (http://www.models.kvl.dk/courses).
[5] R. Bro, Multiway analysis in the food industry: models, algorithms, and applications, Ph.D. Thesis, University of Amsterdam, 1998 (http://www.mli.kvl.dk/staff/foodtech/brothesis.pdf).
[6] R. Bro, Chemom. Intell. Lab. Syst. 38 (1997) 149.
[7] R.D. JiJi, G.A. Cooper, K.S. Booksh, Anal. Chim. Acta 397 (1999) 61.
[8] P.D. Wentzell, S.S. Nair, R.D. Guy, Anal. Chem. 73 (2001) 1408.
[9] D.K. Pedersen, L. Munck, S.B. Engelsen, J. Chemom. 16 (2002) 451.
[10] J.R. Lakowicz, Principles of Fluorescence Spectroscopy, second ed., Kluwer Academic Publishers/Plenum Press, New York, 1999.
[11] R. Bro, N.D. Sidiropoulos, A.K. Smilde, J. Chemom. 16 (2002) 387.
[12] R.D. JiJi, K.S. Booksh, Anal. Chem. 72 (2000) 718.
[13] C.A. Andersson, R. Bro, The N-way toolbox for MATLAB ver. 2.00, Chemom. Intell. Lab. Syst. 52 (1) (2000) 1–4 (http://www.models.kvl.dk).
[14] N.M. Faber, A. Lorber, B.R. Kowalski, J. Chemom. 11 (1997) 419.
[15] A.C. Olivieri, N.M. Faber, Chemom. Intell. Lab. Syst., submitted.
[16] L.A. Currie, Pure Appl. Chem. 67 (10) (1995) 1699–1723.